IOSR Journal of Mechanical and Civil Engineering (IOSR-JMCE)
e-ISSN: 2278-1684,p-ISSN: 2320-334X, Volume 19, Issue 3 Ser. II (May. – June. 2022), PP 37-49
www.iosrjournals.org

Rotational Friction Welding in Dissimilar Steels AISI 1018 – AISI 2225: Effects on Hardness, Fatigue and Microstructure

Víctor Alcántara Alza[1],
[1](Mecánica y Energía/Universidad Nacional de Trujillo, Perú)

Abstract:
The mechanical properties of traction, microhardness, fatigue and microstructure in joints welded by rotational friction (FRW) in dissimilar steels: AISI 1020 and AISI 2205 were studied. The purpose was to observe the behavior of these joints, combining various test parameters.
Specimens for tensile tests according to ASTM E-8, and specimens for Fatigue test according to E466 – 96 were made. The parameters used were: Rotation speed: (1000-1400) rpm; Friction time: (4-6-8) sec; Upset time: 4 sec; Friction Pressure: (3-5) MPa, Upset Pressure: 6 MPa. The tensile tests were carried out on a INSTRON machine of 10 Tn. The microhardness profile was measured longitudinally on the Vickers (HV) scale. Microscopy was performed at the optical level and electronic SEM.
It was found that at 1000 rpm, the highest values of mechanical resistance of the joint are achieved. The maximum value (692.3 MPa) is found with: [n=1000 rpm, Tf= 8 sec, Pf= 5Mpa], giving the joint an efficiency of 103% compared to AISI1020 steel and 70% compared to AISI steel. 2205. The maximum fatigue limit was achieved with: [n=1400 rpm, Tf = 4 sec; Mp = 3 MPa]. Specimens welded at 1000 rpm have a fatigue limit in the range: (225-250) MPa, and those welded at 1400 rpm within: (220-270) MPa. The interface of the weld measures on average ~ 120 µm and the total HAZ zone have on average ~2.2 mm. The joint zone presents severe plastic deformation, and has a fine-grained structure and thickening in the deformation zone.
It is concluded that FRW process, all the parameters influence; they are interdependent variables, and depending on each case, some are more influential than others.
Key Word*: Friction Welding; Fatigue, Mechanical strength, Carbon Steel, Stainless Steel,*

Date of Submission: 08-05-2022 Date of Acceptance: 23-05-2022

I. Introduction

Friction welding is one of the solid states welding methods, that is becoming very important compared to traditional fusion welding methods. During this welding process, heat is generated by conversion of mechanical energy into thermal energy at interfaces during friction under pressure. It is a bonding process in the solid state that produces coalescence in materials using the heat generated between the surfaces rubbing against each other. Under normal conditions the contact surfaces do not melt. No filler metals, flux and shielding gas required in this process. As a general rule, all metallic engineering materials that can be forged can be friction welded; but this process is preferably applied to weld materials of low ductility, because it causes a refinement of the grain; In addition, the heat flow pattern is simple, and residual compression stresses intervene on the surface of these joints that prevent the formation of cracks on the surface **[1].** Friction welding methods are increasingly replacing fusion welding methods, since in the latter, defects such as porosities, residual stresses, fatigue failures, etc. are always found. These defects or failures, in addition to being disadvantageous and affecting the mechanical and physical properties of the joint, cannot be completely eliminated, at best, reduced using complementary methods; such as post-welding heat treatments, which raise production costs. For this reason, friction welding methods have been developed, which in all their forms mitigate the failures of fusion welding **[2].** At present, friction welding is widely used in the automotive and aerospace industries. It is often the only viable alternative in this field to overcome the difficulties found in joining materials with very varied characteristics or dissimilar materials **[3 - 5].** Different methods of joining dissimilar materials have been introduced, both to meet the needs of users and to enhance the added value of new materials while keeping the advantages of existing materials intact. The friction welding method has been found to be the most robust and suitable for mass production, where metals with different components are successfully connected **[6, 7**]. It is an important solution for joining dissimilar materials, due to the particularities of the process, which is based on the conversion of mechanical energy into thermal energy with favorable effects on the resulting interface and the

heat affected zone (HAZ) **[8],** although the quality of the joint depends on the correct selection its welding parameters **[9].**

There are various friction welding techniques; such as rotary friction welding applied to bars and tubes and Friction stir welding applied to plates. In both cases they are used for similar or dissimilar materials, thus solving the problem of materials that had very low weldability. At the beginning it was applied to light materials such as aluminum alloys, titanium and others, where energy consumption was low due to low density; but for a few decades it has been implemented in steels of different grades, similar and dissimilar. Light alloys with steel is also being welding successfully implemented. The use of joints between dissimilar materials has increased considerably and conventional structures made of steel are being replaced by lighter materials, being able to providing high mechanical resistance, less volume of material and good resistance to corrosion, such as the materials used in industries. shipbuilding, automotive, electrical, chemical, civil and nuclear engineering. These components include the joining of parts of different shape and geometry, such as the joining of heat exchanger tubes of different materials, joining of axle boxes and tubes, transmission shafts, drill pipes, electrical connectors, cylinders, pump shafts , pivots, rollers, and so on.. These joints are of great importance because they allow the union of dissimilar components, which in the past were almost impossible to weld by fusion and which is currently possible by friction, as is the case of the welded joints of stainless steel and aluminum components and others **[10]**.

Although friction welding on dissimilar materials has its benefits well established, it should be taken into account that, like any technological process, it also presents certain difficulties that can be summarized in 4 aspects: 1) Composition gradients and microstructural incompatibility between base metals dissimilar properties leading to a wide variation in chemical, physical and mechanical properties in the joint, which can lead to the formation of brittle intermetallic compounds. 2) Associated problems in areas of the joint where there are similarities with the base material. 3) Greater complexity of the joint in the case of needing to add materials used to improve friction. 4) Incompatibility if there are large differences in the physical and chemical properties of the components to be welded **[11].** More than difficulties, they would be recommendations in the friction welding of dissimilar materials. In general, the union of two dissimilar steels can be carried out successfully, as long as the selection of the welding parameters are optimal; this is demonstrated by some of the most advanced research **[12-17].** Ochi et al**. [18]** reported that a higher fatigue limit could be obtained by selecting the correct material group compared to the parent material in joints welded by the friction welding method**.** Celik et al. **[19]** connected the pair of AISI 4140 - AISI 1050 steels by friction welding and reported that the tensile strengths of the metals in the same group were very similar and the changes in hardness in the area under thermal impact varied according to the welding parameters. They also reported that the tensile strength relative to the base material (AISI 1050) was greater than 60%. Satyanarayana et al. **[20],** connected the pair of Austenitic-Ferric stainless steels by the friction welding method and after identifying the most appropriate parameters, they reported that robust welds could only be obtained by combining certain previously studied welding parameters. M. Sahin **[21]** reported that the weld strength of austenitic stainless steel (AISI 304) increased with certain parameters after connecting with friction welding method. Paventhan et al. **[22]** reported that the fatigue resistance of pairs of austenitic stainless steel AISI 304, and medium carbon steel AISI 1040, decreases by applying friction welding methods, a phenomenon that was associated with the characteristics of the microstructure found. They found that the fatigue strength of medium carbon steel joints decreased by 30% and the fatigue strength of austenitic stainless steel decreased by 40% as a result of the welded joint. Radosław W. (2016) **[23],** studied the effect of friction welding parameters on tensile strength and microstructural properties of AISI 1020-ASTM A536 dissimilar steel joints. A hybrid response surface (RSM) and genetic algorithm (GA) methodology was successfully developed to model, simulate and optimize welding parameters. Direct and interaction effects of process parameters on ultimate tensile strength (Rm) were studied by plotting. Friction force and friction time were found to have a positive effect on tensile strength. As the friction force and friction time increase, the tensile strength also increases. The ultimate tensile strength of friction-welded low carbon steel ductile iron joints was 87% of that of the base metal. Furthermore, using energy dispersive spectroscopy (EDS) a carbon distribution was found on both sides of the weld interface. The results of the metallographic study clearly show that the friction welding process was accompanied by a diffusion of carbon atoms from ductile iron into the steel.

The objective of this research is to study the effect produced on microhardness, mechanical properties, fatigue resistance and microstructure, by the union of dissimilar steels: AISI 1018-1025, applying the rotary friction welding method. It is a contribution to the emerging mechanical metal sector.

II. Material And Methods

2.1. Materials

The joints to be welded are made up of two dissimilar steels: Hypoeutectoid carbon steel: AISI 1018 and an austenitic-ferritic stainless steel (Duplex): AISI 2205. Both materials were obtained commercially in the

form of ½" (12.7mm) bars. diameter x 6000mm length; then they were cut on a band saw into bars 80 mm long, and finally they were machined on a parallel lathe to form preliminary specimens ∅12 mm x 75 mm long. The chemical composition was determined using atomic emission spectrometry and the results are shown in table 1.

Table 1. Chemical Composition of the Materials (wt%)

Elements	C	Si	Mn	P	S	Cr	Mo	Ni	Cu	Al	Fe
AISI 1018	0,152	0.344	0.872	0.023	0.006	0.031	0.004	0.026	0.017	0.044	Bal.
AISI 2205	0.018	0.300	1.680	0.024	0.003	22.886	3.368	4.892	0.095	-	Bal.

2.2. Welding Parameters.

Friction welding (FRW) test parameters are shown in Table 2. These parameters include friction pressure, friction time, friction speed and forging pressure, which have a great influence on the process. welding **[24–27].** Table 3 shows the matrix of tests making a random distribution, where 12 tests with 2 repetitions would result, which indicates that 24 specimens would be used, of which only one would be selected; the one with the best welded joint giving rise to 12 samples presented.

Table 2. Essays parameters and their levels which the welding was executed

Parameters	**datas**	**levels**
Rotation Speed (rpm)	1000-1400	2
Friction Time (s)	4-6-8	3
Upset Time (s)	4	Constant
Friction Pressure (MPa)	3-5	2
Upset Pressure (MPa)	6	Constant

Tabla 3. FRW welding parameters, indicated for each welded sample with its nomenclature.

Sample:	**P1**	**P2**	**P3**	**P4**	**P5**	**P6**
Rotation Speed (rpm)	1000	1000	1000	1000	1000	1000
Friction Time (s)	4	6	8	4	6	8
Upset Time (s)	4	4	4	4	4	4
Friction Pressure (MPa)	3	3	3	5	5	5
Upset Pressure (MPa)	6	6	6	6	6	6
Sample:	**P7**	**P8**	**P9**	**P10**	**P11**	**P12**
Rotation Speed (rpm)	1400	1400	1400	1400	1400	1400
Friction Time (s)	4	6	8	4	6	8
Upset Time (s)	4	4	4	4	4	4
Friction Pressure (MPa)	3	3	3	5	5	5
Upset Pressure (MPa)	6	6	6	6	6	6

2.3. FRW Welding

For the FRW welding tests, the equipment shown in Figure 1 had to be designed and implemented. The details of the mechanism are shown in the Figure. The welding was by Direct Impulse. One of the pieces is attached to the mobile chuck "C" driven by motor "B"; while the other to the "D" chuck, restricting its movement so that it cannot rotate during the test and friction occurs.

Each sample is mounted on both chucks and rotates until reaching the parameters programmed and controlled by PLC "A" which is coupled to motor B by a cable. At the end of the friction time, the motor is blocked so that the piece stops turning and then the pressure and upset time are applied, using the hydraulic device coupled to a pressure sensor "F" with a reading manometer.

The tests were performed for each sample, programming the equipment for each of them according to the parameters specified in Table 3.

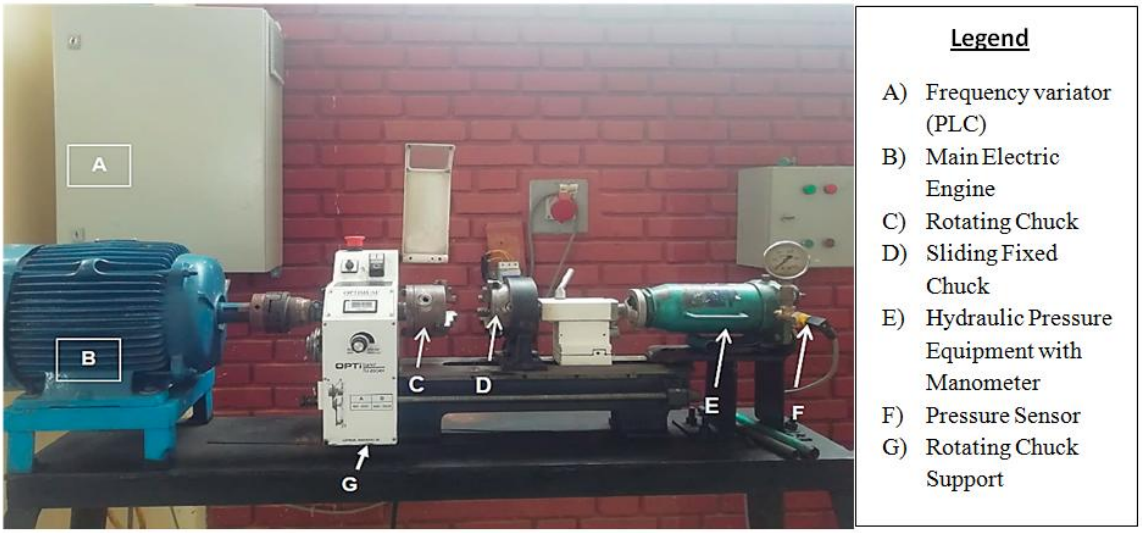

Figure 1. Rotary Friction welding Setup.

2.4. Microhardness

The microhardness tests were carried out using the Vickers CV400AAT trademark microhardness tester. Measurements were made by applying a load of 10 Kg using a diamond pyramid with a base angle of 136º as indenter; following the ASTM 384 standard. Before carrying out this test, the welded specimens had to be cut by the central surface and then rectified and polished on their flat surface to guarantee the measurement. Measurements were made with a spacing of 0.5 mm, taking 5 points on each side of the center line.

2.5. Traction and Fatigue Essays

The tensile tests were carried out in the TECNCTEST tensile testing machine with a capacity of 10 tons. These tests were carried out following what is typified in the ASTM E8 standard. The specimens used were machined following the outline of the sketch in figure 2 (a). Before testing these samples had to be ground and polished in the 26 mm test zone, to arrive at a tolerance setting Ø6 ±0.05.

The Fatigue Tests were carried out by the rotary bending method. A Moore machine designed for this purpose was used. During operation an electric motor rotates a cylindrical specimen at 1800 RPM and a simple counter records the number of cycles. The loads are applied in the center of the specimen, with a rotation system. It also handles a switch, which stops the test at the moment the fracture is caused and the weights descend. All the samples, of specified length, were subjected to the machine with a frequency of 100 Hz and a stress ratio: R = -1

The scheme of the specimens used is shown in figure (2b). We must take into account that the ASTM E466 standard specifies all the details of the specimens used in the axial fatigue tests. However, for rotary bending tests, there is no specification by the ASTM, nor in the type of machine to be used. The specific dimensions of the specimens depend on the experimental objective, the machine in which it is to be used, and the material available. The ASTM only specifies the preparation techniques, details and technical reports. The details of the sample presented in figure 2b) have been obtained from the reports of other studies already carried out. The tolerances in the central test area are the same as those shown on the tensile specimens.

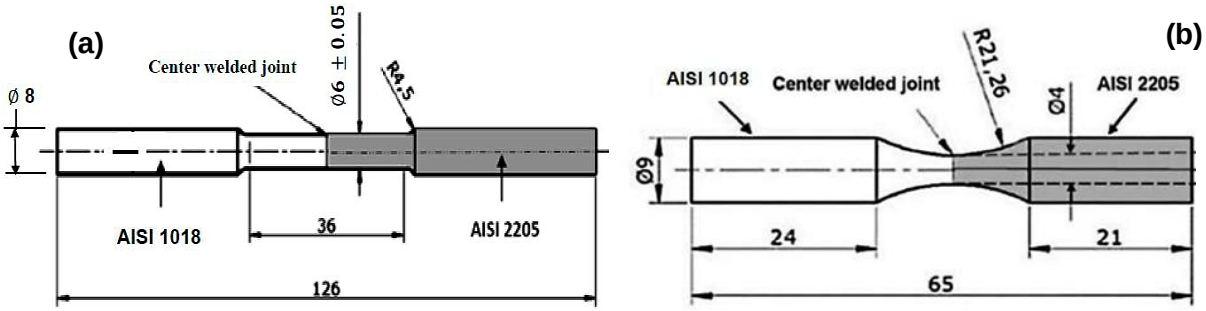

Figure 2. Sketch showing measurements for Tensile test specimens (a); Fatigue test specimens (b)

2.6. Microscopy Essays

The microscopy analysis was done at the optical and electronic level.

To reveal the microstructure at the optical level, the Zeiss 1000X microscope was used. Before revealing the microstructure, the sample surfaces were roughened, polished and chemically etched. These were then encapsulated in metal molds to achieve a flat surface. Sandpaper from grade 220 to 1000 was used, then these samples were polished with corduroy cloth coated with alumina from grade 5 µ, 3 µ, 1 µ, up to 0.3 µ and water for 30 seconds. Subsequently, they were attacked with Nital 2% for 60 seconds, being ready to take them to the microscope and reveal their microstructure. 2 photomicrographs were taken for the samples as supplied.

For the microstructure at the electronic level. The equipment 30 KV JEOL brand scanning electron microscope (SEM) was used. With this equipment, 6 microphotographs were taken of the welded samples. The first 3 (P1→P3). welded at 1000 rpm were taken at low magnifications to observe the HAZ zones. The next three (P7→P9) welded at 1400 rpm were taken at higher magnifications to be able to observe the microstructure in the joint zone. It was not necessary to show all the other samples because they follow almost the same pattern.

III. Result

3.1. Microharness

For the materials as supplied, an average hardness of 112 HV was found for AISI 1018 steel and a hardness of 205 HV for AISI 2205 steel. The microhardness profiles for all welded joints are plotted in Figure 3. The side left corresponds to AISI 1018 steel and the right side to AISI 2205 steel.

Regarding the trend values and comments on these profiles will be made in item IV corresponding to the Discussion.

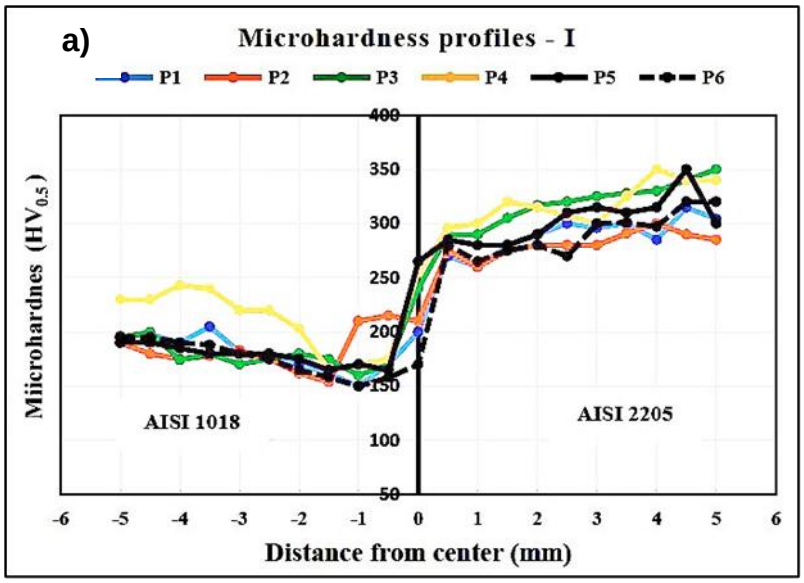

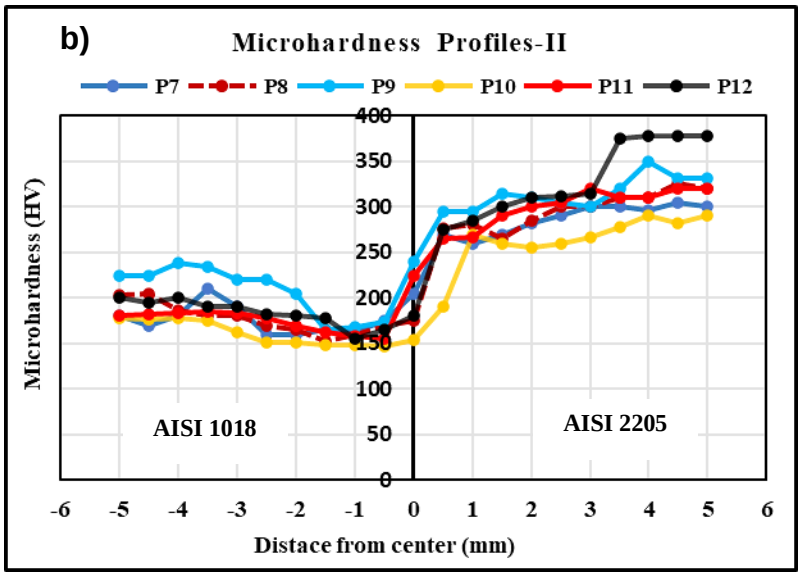

Figure 3. Microhardness profiles of FRW-welded joints; a) For samples welded at 1000 rpm. b) For samples welded at 1400 rpm.

As a whole, it can be seen that the trends of both profiles are similar, finding that only the values change slightly with the speed of rotation. More details will be given later.

3.2. Maximum Tensile Strength (Rm)

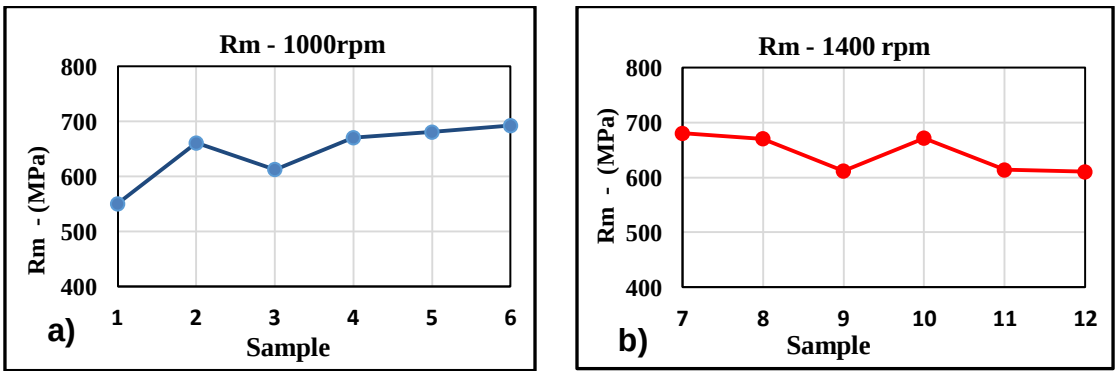

Figure 4. Graphs showing the trend of the maximum tensile strength. Each dot represents the sample number. a) For samples tested at 1000 rpm, b) For samples tested at 1400 rpm

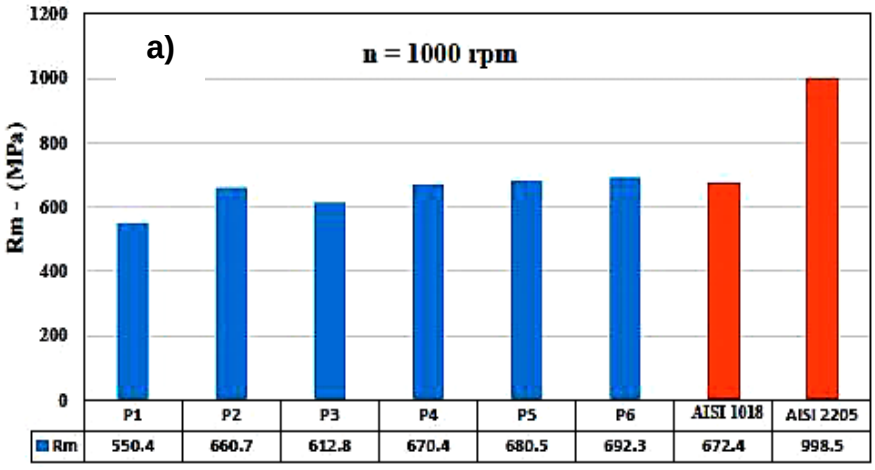

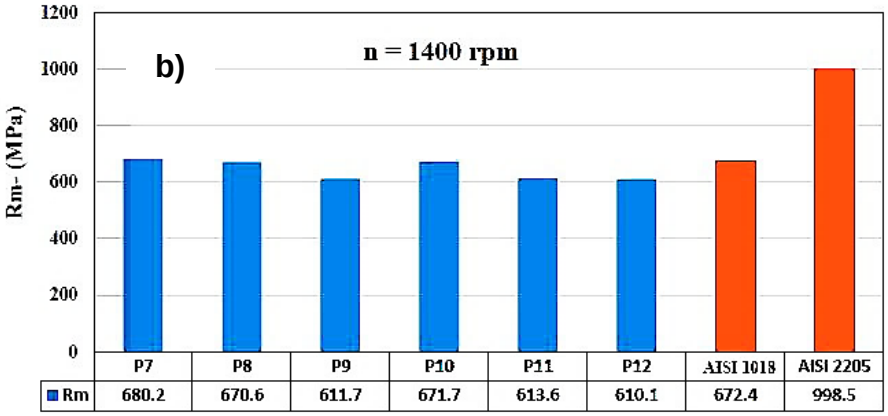

Figure 5. Graphs showing the Rm values obtained in the tensile tests, a) For samples welded at 1000 rpm, b) For samples welded at 1400 rpm.

3.3. **S-N Diagrams of Fatigue Resistance**

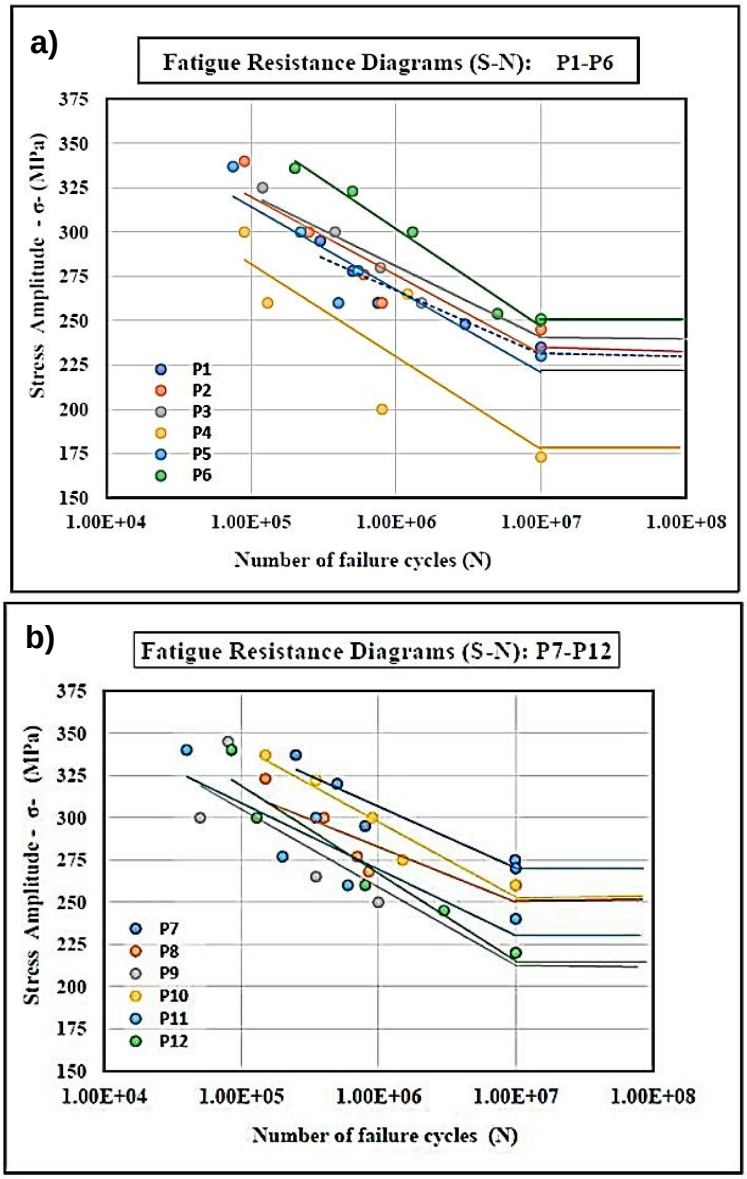

Figure 6. Rotational fatigue S-N graphs of samples welded with FRW a) For samples welded at 1000 rpm, b) For samples welded at 1400 rpm.

3.4. Endurance Limits for Welded samples (σ'_f)

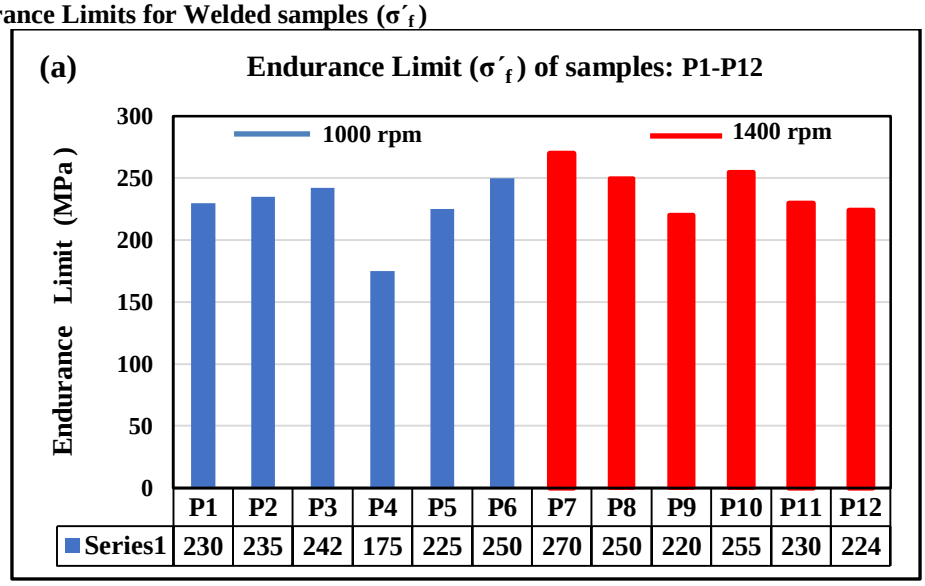

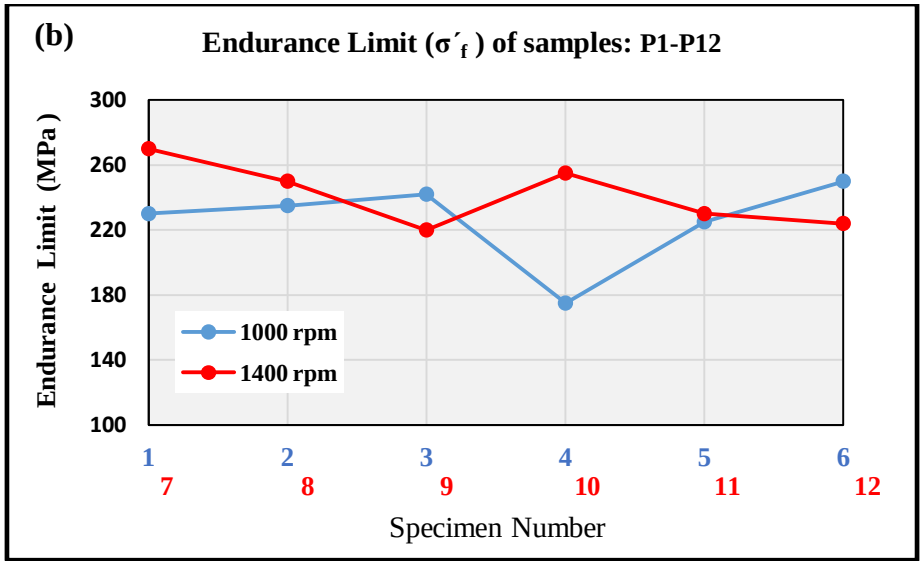

Figure 7. Graphs showing the endurance limits for welded samples a) Graph showing the values of σ'_f ; b) Graph showing the variation of the fatigue limit for the samples welded: a) 1000 rpm; (P1-P6); b) 1400 rpm (P7-P12)

3.5. microstructure

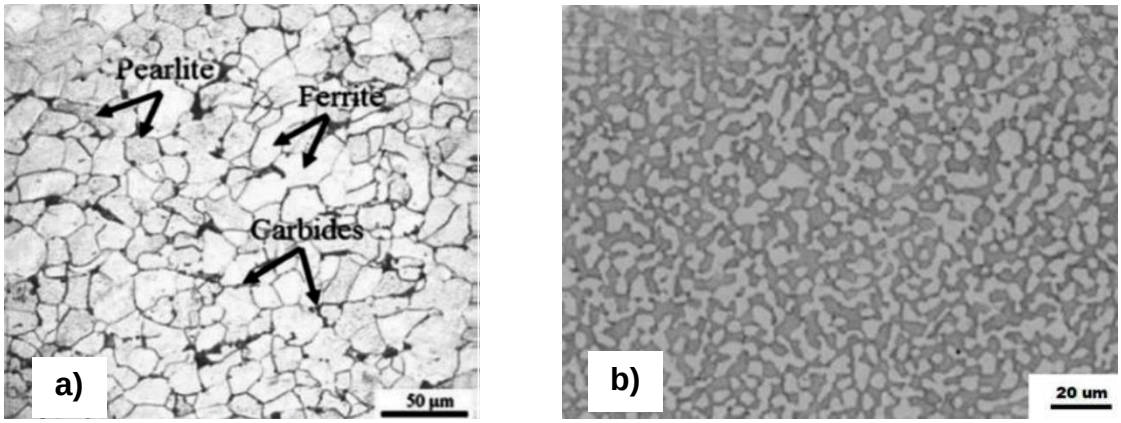

Figure 7. Optical microstructures of the samples as supplied; a) AISI 1018; B) AISI 2205

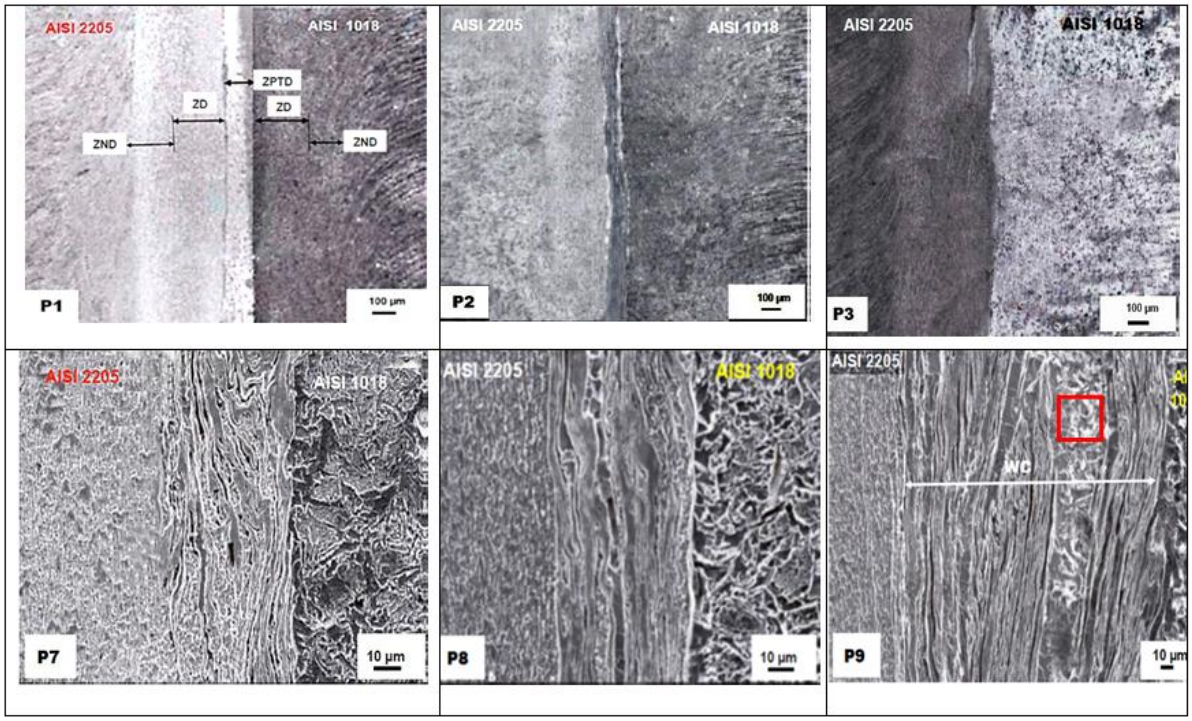

Figure 8. SEM microstructures showing details of the surroundings of the junction: central zone (ZPTD) and deformed (ZD) and undeformed (ZND) zones. P1), P2) and P3) correspond to joints welded at 1000 rpm; P7), P8), P9), correspond to joints welded at 1400 rpm. The latter show internal details of the central zone (ZPTD).

IV. Discussion

a) Maximum Tensile Strength (Rm)

The results and trend graphs are shown in Fig. 4 and Fig.5 The maximum value of Rm (692.3 MPa) is presented by sample P6, welded with the following parameters: [1000 rpm, Tf= 8 sec, Pf= 5Mpa]; corresponding to the lower speed, longer friction time and higher friction pressure. The minimum value of Rm (550.4 MPa) corresponds to sample P1, welded with the following parameters: [1000 rpm, Tf= 4 sec, Pf= 3Mpa], corresponds to the lowest speed, the lowest friction time, the lowest friction pressure. It is noteworthy to note that both the minimum and maximum value of Rm are found within the samples welded with the lowest speed (1000 rpm), which indicates that the greatest effect on Rm is defined by friction pressure and friction time. Taking the maximum value of Rm, the efficiency of the joint is 70%, compared to AISI 2205, which is the most resistant base material.

The Rm values of the samples welded at 1000 rpm do not differ much from AISI 1018 steel. The maximum value is 692.6 MPa and corresponds to sample P6, being a value greater than that corresponding to the base material with a difference in excess $\Delta = 20$ MPa. For the samples with this rotation speed, it is observed that the Rm values are higher and lower than the Rm of the base metal AISI 1018; but with respect to AISI 2205 steel, all the Rm values are much lower, reaching a difference of up to $\Delta = 338$ Mpa. For the samples welded at 1400 rpm, a similar behavior is observed. The trend curves of all the welded samples are irregular. For 1000 rpm, Rm shows a slight tendency to growth; on the other hand, for 1400 rpm the trend is slightly decreasing.

In the results, for the two rotation speeds, high and low values of Rm are observed, even these values overlap. Therefore, it follows that for this property this parameter is not very influential; observing that the most influential parameters are the pressure and friction time (Pf and Tf) as long as the forging time and pressure are kept constant. These results are in agreement with the studies of R. Winiczenko **[28],** where it is concluded that the friction force and the friction time have a very positive effect on the tensile strength in steel and cast iron joined by Rotational Friction. . As the friction force and friction time increase, the tensile strength also increases according to C. Ellis **[29],** as the friction welding pressure increases, within certain limits, the tensile strength Rm of the weld increases, approaching the base metal.

In the present research, the upsetting pressure has remained constant; but it should be noted that this pressure has a negative effect on the tensile strength. As upsetting pressure increases, tensile strength decreases. mainly due to stress-induced deformation as reported by T. Udayakumar et al**. [30].**

b) S-N Diagrams and Endurance Limits

The S-N graphs of all the samples tested are found in Figure 6 and the graphs of the endurance limits are found in figure 7. The results are shown in Fig. 6, and Fig.7 corresponding to all samples. Figure 6a) shows the S-N diagrams for the samples welded at 1000 rpm and 6b) shows the S-N diagrams for the samples welded at 1400 rpm. All the samples have endurance limit. Sus valores y diagramas se pueden ver en la figura 7. The maximum value of endurance limit is 270 MPa corresponding to the sample P7 [1400 rpm, Pf = 3 MPa, Tf = 4s]. The minimum value is 175 MPa corresponding to sample P4 [1000 rpm, Pf = 5 MPa, Tf 4s]. In the samples welded at 1000 rpm, the variation of endurance limit is in the range (230-250) MPa and a growing trend is observed, with the exception of sample P4. Considering the statistical nature of fatigue (its randomness), there is a high probability that the data from test piece P4 is out of control, since it does not agree with the trend of values found. If we leave this value without effect, the trend of endurance limit would be increasing (almost linear); that is, with this parameter of 1000 rpm, the fatigue limit increases with the friction pressure and friction time, keeping the upset time and upset pressure constant. In figure 6b) the S-N curves for the specimens welded at 1400 rpm show the endurance limits within the range (270-224) MPa, showing a decreasing trend. For the samples tested at 1000 rpm and without considering the value supposedly out of control, the interval would be (230-250) MPa. The parameter changes would produce an increase on endurance limit of $\Delta\sigma'f = 20$ MPa. For the samples tested at 1400 rpm, without taking into account out of control points, the interval would be (270-224) producing a decrease on endurance limit of $\Delta\sigma'f = 36$ MPa.

Summarizing: For all samples with constant upset pressure and upset time parameters it is had the following:

Maximum endurance limit: 270 MPa (sample P7): [n=1400 rpm, Tf= 4 sec; Mp= 3MPa]

Minimum endurance limit: 175 MPa (sample P4): [n= 1000 rpm, Tf= 4 sec; Mp= 5 MPa]

For a better description of the results, figure 9 has been added, showing the trend curves of the fatigue limits

for both speeds. In the first case (1000 rpm) they show a slightly increasing trend and in the second case, the trend is

sharply decreasing. This shows that although the most significant parameters are pressure and friction time (Pf; Tf). It follows that the change in speed, plays a very important role; Therefore, speed is the variable that determines the heat supplied to the joint to a greater degree. In the first case, the variation would be justified by the lower rotation speed and the increase in friction pressure. In the second case, the decrease would be justified by the increase in rotational speed and the increase in friction time. Hasalik and Ozdemir **[31]** investigated the fatigue behavior of a friction-welded AISI 304 stainless steel and AISI 4340 dissimilar joint and found that the fatigue strength decreased with increasing rotational speed as a result of precipitate formation of chromium carbide at the weld interface, to which the reduction of the endurance limit is attributed .

When it comes to the statistical nature of fatigue, it is reported that fatigue tests are very difficult to quantify when using small numbers of samples. For some time up to now, there has been considerable interest in analyzing the reasons for variability in fatigue test results; Therefore, it has become necessary to have a statistical approach so that the fatigue data can be adequately evaluated. Otherwise, each test would need a considerable number of specimens to obtain precise or exact data **[32].** This is the reason why the trend curves of figure 9 have been added. If the values of the endurance limit are irregular, the trends are not so irregular, due to the statistical nature of fatigue.

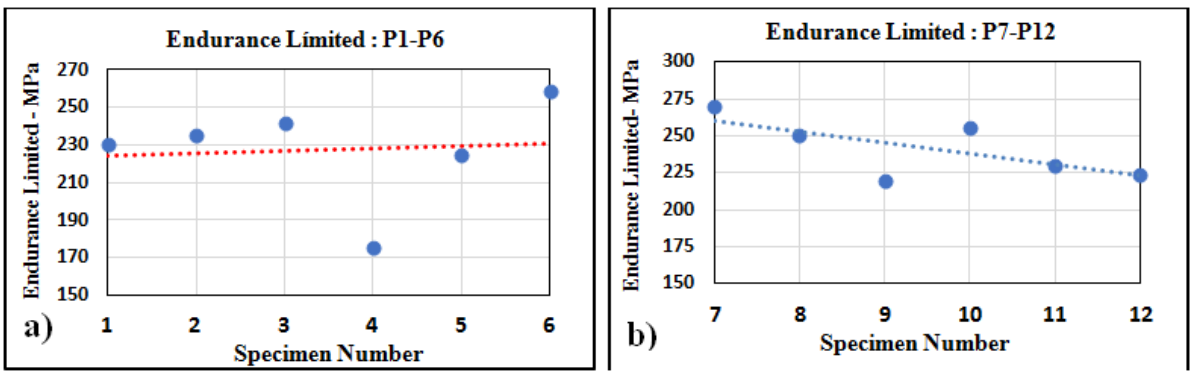

Figure 9 . Graphs showing the endurance limits with their respective trend curves with linear fit; a) For samples welded at 1000 rpm, b) For samples welded at 1400 rpm.

c) Microhardness Profiles

Microhardness profiles of joints welded at 1000 rpm. and 1400 rpm are shown in figure 3. All measurements have been made in a range: (-5; +5) mm; that is, in a thickness of 10 mm, to ensure that we are in an area corresponding to the entire HAZ or approximately. In the profiles of all the samples, greater hardness is observed in the area corresponding to AISI 2205 steel compared to AISI 1018 steel. The maximum value of the samples welded at 1000 rpm is 350 HV and it is found in the AISI 2205 area in three samples: P3 (x= +5mm), P4 (x= + 4mm) and P5 (x= +4.5mm). For samples welded at 1400 rpm in the same area, the maximum value is 378 HV belonging to sample P12 (x= +4 mm). The difference between these two peak values is Δ= 28 HV, which means an increase of 8%, in this area due mostly to change in rotational speed and also due to the change in pressure and friction time.

Considering the hardness of the base materials of 112 HV for AISI 1018 and 205 HV for AISI 2205, the maximum hardness of the joint zone represents an increase of 85% with respect to AISI 2205 and 154% with respect to AISI 1018, which This means that there are zones of hardening in the weld interface and surroundings that are very hardened with respect to the base metals, which would give rise to zones of possible cracking, which would recommend applying a post-weld heat treatment to reduce the existing residual stresses that have been generated.

The central line or union zone presents different hardness for each sample, due to the change in the welding parameters. The results and trends can be seen in the graphs of Figure 10, where it is observed that for the samples welded at 1000 rpm, there is an increasing trend in the values, except for test sample P6.

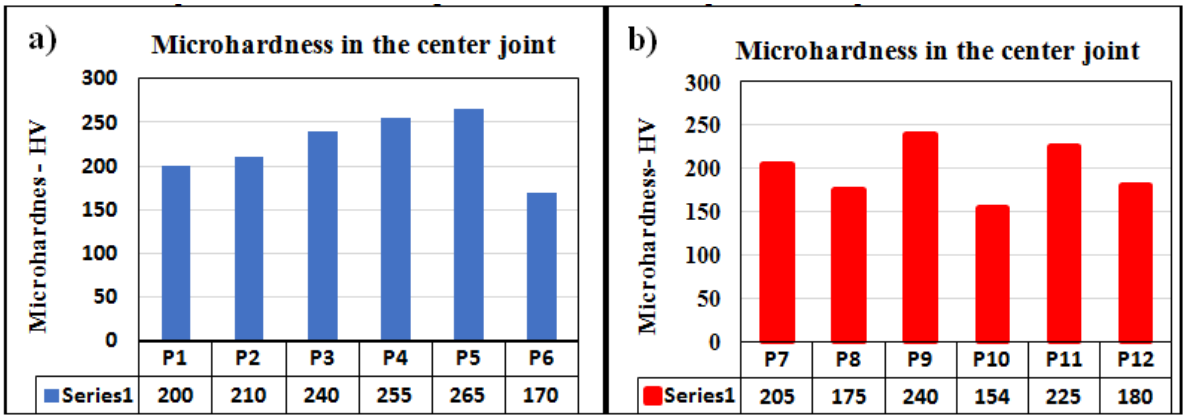

Figure 10 . Microhardness graphs in the center joint; a) For samples welded at 1000 rpm, b) For samples welded at 1400 rpm.

For the samples welded at 1400 rpm, a very irregular pattern of hardness is observed; presenting oscillating values. These hardness changes at the weld interface are directly associated with the microstructure resulting from the degree of heat that is introduced and the plastic deformation **[33, 34].**

Hardness profiles shown in the graphs of figure 3 show the following: Regarding AISI 2205 steel, the general tendency of hardness is to increase from the central line of the cord towards the base metal, and with respect to AISI 1018 steel there is no defined trend, since its values are highly oscillating.

d) Microestructure

The microstructure of the steels as supplied is shown in Figure 7. AISI 1018 steel shows a pearlitic-ferritic structure with certain fine nucleated carbides at the grain boundaries. For AISI 2205 steel, a fine-grained Duplex structure formed by Austenite + Ferrite is observed, characteristic of these stainless steels.

The microstructure of the friction-welded specimens can be found in Figure 8. Specimens P1, P2 and P3 (welded at 1000 rpm) are shown at moderate magnification so that the areas that make up the entire HAZ can be seen. Then the microstructure of samples P7, P8, P9 (welded at 1400rpm) are presented at higher magnifications to observe the details of the joint zone.

Rotational friction welding has as its main disadvantage, the rate of heat generation is not uniform over the interface. This gives rise to a non-uniform thickness of the heat-affected zone (HAZ), for which a minimum or optimum thickness cannot be found at all points of the interface. According to M. Maalekian **[35],** the thickness is not constant. The high temperature gradient available in the junction zone explains why there is a very small HAZ in this process. On the other hand, due to the narrowness of the HAZ, the welding distortion is kept to a minimum **[35],** which can be considered as an advantage of the process.

As stipulated in reference **[36],** the ZAC, in FRW rotary friction welding, can be divided into four (4) zones:

I. Contact zone **(ZPTD):** Zone of severe plastic deformation (contact zone). It is a fully deformed zone and has a very fine grain structure due to severe stress and complete recrystallization.
II. Deformed Zone **(ZD):** This zone has a very fine grain structure due to severe deformation and complete recrystallization. The grains in this zone are fine and equiaxed.
III. Partially Strained Zone **(PDZ):** The microstructure becomes coarser due to the associated reduction in strain amount and strain rate.
IV. Non-deformed zone **(ZND).** In this region, the steel can undergo a phase transformation without plastic deformation occurring. Grain growth can take place.

Outside these zones is the base material **(MB).** The nomenclature is located in sample P1 of figure 8. Depending on the scale of the photomicrographs we can give some approximate measurements on average. The measurements made on the P2 specimen were taken as a model, and the following thicknesses were found:
ZPTD ~ 120 µm; ZD ~ 880 µm; ZPD ~ 300 µm; ZND ~ 900 µm; making the total sum the thickness of the HAZ would be ~2.2mm, which is quite a thin thickness compared to fusion welding processes. The remaining specimens present measurements not very far from the one obtained for P2. Regarding the microstructure, it has been observed that the granular structure follows the rules of ref**. [36].**

In the microstructures of specimens P7, P8 and P9 taken at higher magnifications, the ZPTD interface zone is observed in detail. A fully plasticized zone is observed but with varied recrystallization. In the P9 microstructure, a zone with marked dynamic recrystallization (marked with a red rectangle) is clearly observed. It can be concluded that the joint zone in all the samples presents a severe plastic deformation, but degree of recrystallization is not the same in each of them due to the varied welding parameters used in each sample. These parameter variations produce a different heat input, giving rise to the samples having different degrees of recrystallization in the interface zone.

V. Conclusion

After carrying out an experimental study on the Effects on Hardness, Fatigue and Microstructure of dissimilar welded joints of AISI 1018 - AISI 2225 steels applying the FRW method, the following conclusions are drawn:

1. The maximum value of mechanical resistance (Rm) is 692.3 MPa and is presented by test sample P6, welded with the parameters: [1000 rpm, Tf= 8 sec, Pf= 5Mpa]. The efficiency of the joint reached 70%, compared to AISI 2205, which is the most resistant base material.
2. The results show that the lower rotation speed presents higher values of Rm; In addition, the most influential parameters are the pressure and friction time (Pf and Tf) as long as the upset time and upset pressure are kept constant.
3. All samples presented their endurance limit at $1.0x10^7$ cycles. The maximum value of the endurance limit is 270 MPa corresponding to the sample P7 [1400 rpm, Pf = 3 MPa, Tf = 4s]. The minimum value is 175 MPa corresponding to sample P4 [1000 rpm, Pf = 5 MPa, Tf 4s].
4. The endurance limit decreases with increasing rotational speed, probably as a result of the formation of chromium carbides at the joint interface.
5. The maximum value of the hardness in the samples welded at 1000 rpm is 350 HV. For samples welded at 1400 rpm, the maximum is 378 HV. The difference between these two peaks is Δ= 28 Hv, which represents an 8% increase, due in part to the change in rotational speed.
6. The maximum hardness at the interface of the joint represents an increase of 85% with respect to the base material AISI 2205 and 154% with respect to AISI 1018, which means that there are specific areas of hardening in the interface, probably due to the formation of carbides chrome above mentioned.
7. The microstructures reveal quite thin widths for the different HAZ zones of order of microns, and the interfaces present severe plastic deformation, but the degree of recrystallization is not the same in each of them, due to the different welding parameters used for each sample.
8. Finally, it is inferred that in this FRW friction welding process, all the parameters influence; they are interdependent variables, and depending on the test case, some of them are more influential than others.

References

[1] Radosław W., Mieczysław K., Friction welding of ductile iron with stainless steel, Journal of Materials Processing Technology 213 (2013) 453– 462
[2] Sahin M., Akata H., Gulmez T., Characterizacion of mechanical properties in AISI 1040 parts welded by friction welding, Materials Characterization, Volume 58, p.p 1033-1038, September 2006.
[3] Gurler M. Friction welding characteristics of aluminum alloy. PhD. Thesis. Marmara University, Institute of Science, Istanbul; 2000.
[4] Kırık I, Ozdemir N, Sarsılmaz F. Microstructure and mechanical behaviour of friction welded AISI 2205/AISI 1040 steel joints. Mater Test 2012; 54(10):683–7

[5] Mitelea I., Budau V. ,Craciunescu C., «Dissimilar friction welding of induction surface hardened steels anda thermochemically treated steels,» Journal of Materials Processing Technology, 2012.

[6] Atehortua-López. D.F., "Porpagación de grietas en uniones soldadas por FCAW de aceros de bajo carbono y aceros de baja aleación y la aplicabilidad del ultrasonido como herramienta de monitoreo en este tipo de estudios", PhD. Tesis, Facultad de Ingeniería, Universidad del Valle, Cali, Colombia, 2016

[7] Uzkut M., Unlu B.S., Yilmaz S.S., Akdağ M..; Friction Welding And It Applications in Today´s World. available in: http://eprints.ibu.edu.ba/621/1/issd2010_science_book_p710-p724.pdf

[8] Dinc D. Investigation of weldability of AISI 1020 and AISI 304 steels by friction welding. M.Sc. Thesis. Balıkesir University, Institute of Science, Balıkesir; 2006.

[9] A. W. Society, Manual de Soldadura, Tomo III. AWS, 1996.

[10] Akata H., «Joining with friction welding of plastically deformed steel.»

[11] Tauzi M.A., Zuhailawati H., Ismail, A.«A review: Advances in friction welding process.».

[12] Ma H, Qin G, Geng P, Li F, Fu B, Meng X, Microstructure characterization and properties of carbon steel to stainless steel dissimilar metal joint made by friction welding, Materials and Design 2015;86:587-597.

[13] Nathan S.R, Balasubramanian V, Malarvizhi S, Rao A.G, An investigation on metallurgical characteristics of tungsten based tool materials used in friction stir welding of naval grade high strength low alloy steels, International Journal of Refractory Metals and Hard Materials 2016;56:18-26.

[14] Li X, Li, Liao Z, Jin F, Zhang F, Xiong J, Microstructure evolution and mechanical properties of rotary friction welded TC4/SUS321 joints at various rotation speeds, Materials and Design 2016;99:26-36.

[15] Reilly A, Shercliff H, Chenb Y, Prangnell P, Modelling and visualisation of material flow in friction stir spot welding, Journal of Materials Processing Technology 2015;225:473-484.

[16] Sarkara R, Pala T.K., Shome M., Material flow and intermixing during friction stir spot welding of steel, Journal of Materials Processing Technology 2016;227 96-109.

[17] Kurt B., The interface morphology of diffusion bonded dissimilar stainless steel and medium carbon steel couples, Journal of Materials Processing Technology 2007;190:138-141.

[18] Ochi H, Yamamoto Y, Ogawa K, Tsujino R, Sawai T, Suga Y. Evaluation of tensile strength and fatigue strength of SUS304 stainless steel friction welded joints. Int Soc Offshore Polar Eng Conf 2003:1098–6189

[19] Celik S, Ersözlü _I. Investigation of the mechanical properties and microstructure of friction welded joints between AISI 4140 and AISI 1050. Mater Des 2009;30:970–6.

[20] Satyanarayana VV, Reddy MG, Mohandas T. Dissimilar metal friction welding of austenitic–ferritic stainless steels. J Mater Process Technol 2005;160(2):128–37

[21] Sahin M. Evaluation of the joint interface properties of austenitic-stainless steels (AISI 304) joined by friction welding. Mater Des 2007; 28:2244–50.

[22] Paventhan R, Lakshminarayanan PR, Balasubramanian V. Fatigue behaviour of friction welded medium carbon steel and austenitic stainless steel dissimilar joints. Mater Des 2011;32:1888–94.

[23] Radosław W. "Effect of friction welding parameters on the tensile strength and microstructural properties of dissimilar AISI 1020-ASTM A536 joints", Int J Adv Manuf Technol (2016) 84:941–955, Springerlink

[24] Sahin M, Akata HE. An experimental study on friction welding of medium carbon and austenitic stainless steel components. Ind Lubr Tribol 2004;3(56):122–9.

[25] Ananthapadmanaban D, Rao VS, Abraham N, et al. A study of mechanical properties of friction welded mild steel to stainless steel joints. Mater Des 2009;30(7):2642–6.

[26] Paventhan R, Lakshminarayanan PR, Balasubramanian V. Optimization of friction welding process parameters for joining carbon steel and stainless steel. J Iron Steel Res Int 2012;19(1):66–71.

[27] Ma H, Qin G, Geng P, et al. Microstructure characterization and properties of carbon steel to stainless steel dissimilar metal joint made by friction welding. Mater Des 2015;86:587–97.

[28] Winiczenko R. Effect of friction welding parameters on the tensile strength and microstructural properties of dissimilar AISI 1020-ASTM A536 joints, Int J Adv Manuf Technol (2016) 84:941–955

[29] Ellis CRG (1972) Continuous direct drive friction welding of mild steel. Weld Res Suppl 4:183–197

[30] Udayakumar T, Raja K, Afsal Husain TM, Sathiya P (2014) Prediction and optimization of friction welding parameters for super duplex stainless steel (UNS S32760) joints. Mater Des 53:226–235

[31] Hasalik A, Ozdemir N. Fatigue behavior of AISI 304 steel to AISI 4340 steel welded by friction welding. J Mater Sci 2006;41:3233–9

[32] Dieter G.E.. Mechanical Metallurgy, McGRAW-HILL Book company,1961, pp: 301-302

[33]. Kurt A, Uygur I, Paylasan U (2011) Effect of friction welding parameters on mechanical and microstructural properties of disimilar AISI 1010-ASTM B22 joints. Weld J 90:102–106

[34]. Sathiya P, Aravindan S, Noorul Haq A (2007) Effect of friction welding parameters on mechanical and metallurgical properties of ferritic stainless steel. Int J Adv Manuf Technol 31:1076–1082

[35] Maalekian M., Friction welding–critical assessment of Literatura-Review Science and Technology of Welding and Joining 2007 VOL 12 N° 8 -738.

[36] Mercan S., Ozdemir N., A couple of AISI 2205/AISI 1020 Material Combination with Friction Welding Method, NWSA-Technological Applied Sciences, 2A0080, 8 (2013) 2, 18–34, doi:10.12739/ NWSA.2013.8.2.2A0080

Víctor Alcántara Alza. "Rotational Friction Welding in Dissimilar Steels AISI 1018 – AISI 2225: Effects on Hardness, Fatigue and Microstructure". *IOSR Journal of Mechanical and Civil Engineering (IOSR-JMCE)*, 19(3), 2022, pp. 37-49.